Dislocation-mediated melting near isostructural critical points

T. Chou[1] and David R. Nelson[2]
[1]*Laboratory of Atomic and Solid State Physics, Cornell University, Ithaca, New York 14853*
[2]*Department of Physics, Harvard University, Cambridge, Massachusetts 02138*
(Received 26 September 1995)

We study the interplay between an isostructural critical point and dislocation-mediated two-dimensional melting, using a combination of Landau and continuum elasticity theory. If dislocations are excluded, coupling to the elastic degrees of freedom leads to mean-field critical exponents. When dislocations are allowed, modified elastic constants lead to a phase buried in the solid state near the critical point. Consistent with a proposal of Bladon and Frenkel [P. Bladon and D. Frenkel, Phys. Rev. Lett. **74**, 2519 (1995)], we find an intervening hexatic phase near the critical point of the first-order isostructural transition line. Very close to the critical point, a transition from the hexatic phase to a modulated-bond-angle state is possible. Ising transitions in symmetrically confined two-dimensional colloidal crystals with attractive wall potentials require a different model free energy, which we also discuss.

PACS number(s): 82.70.Dd, 68.35.Rh, 61.72.Lk, 64.70.Kb

I. INTRODUCTION

First-order phase transitions preserving symmetry and possessing a critical point have been well understood for many years, the most common example being the discontinuous liquid-vapor phase transition. Such systems can be brought continuously from one phase to another by taking a thermodynamic path that passes around the critical point along the equation of state surface without sudden changes in density. Near the critical point, liquid-vapor systems show critical opalescence, among other properties, peculiar to second-order phase transitions.

Recently, attention has been focused on *solid-solid* phase transitions [1–3]. Especially interesting are isostructural transitions in which the lattice spacing jumps discontinuously, but the symmetry of the lattice remains unchanged. A schematic phase diagram as a function of temperature T and particle density ρ is shown in Fig. 1. As in the liquid-vapor transition, isostructural transitions can have a critical point above which the distinction between the isostructural phases S_1 and S_2 vanishes. Because the solid-solid coexistence region is on the higher density (solid) side of the fluid-solid coexistence region, a fluid-solid-solid triple point becomes possible.

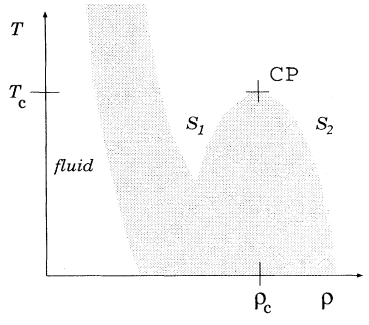

FIG. 1. T-ρ phase diagram of a system exhibiting a solid-solid phase coexistence. CP is a critical point and S_1 and S_2 are the low- and high-density solids, respectively.

Experimentally, bulk isostructural transitions have been observed in high-pressure studies of Zr. Above the fcc to ω (at 6.7 GPa) and ω to bcc (at 33 GPa) transitions, a lattice symmetry-preserving transition between two bcc phases occurs at 53 GPa [4]. Another experimentally convenient system with which to study solid-solid transitions is colloidal particles. Colloids are often observed to be in an ordered fcc or bcc lattice, useful, for example, in colloidal array filters [5]. The interaction potential between colloid particles can be chemically tailored to control the range of interactions. For example, one can vary the length of grafted polymers or change solvent properties [6]. Single layers of colloids can be confined to study the transitions of two-dimensional (2D) solids [7]. This has been achieved by squeezing colloidal particles between two flat plates [8] or floating them at an air-water interface [9].

The theoretical study of the statistical mechanics of colloidal particles has utilized various analytical [3,10–12] and numerical [13,14] methods. It is well established that hard spheres, with or without a superimposed attractive potential, can undergo a solid-fluid phase transition. When the attractive potentials are short ranged enough, experiments and theory demonstrate that the liquid-gas coexistence vanishes [14,15]. The short-ranged attractive potentials required can be achieved with colloidal particles or in computer simulations. A recent numerical study [2] using particles with very short-ranged attractive potentials (attractive region less than 7% of the hard-core diameter) and at high densities show solid-solid phase coexistence. This behavior is consistent with the variational treatment of Tejero *et al.* [3].

In this paper, we explore how defect mediated melting [16] may be incorporated into the schematic phase diagram of particles with short-ranged attractions. There is some evidence for a two-stage dislocation-mediated melt-

ing process in liquid crystals [17], colloidal dispersions [8], and magnetic bubble domains [18]; however, a first-order transition from solid to liquid (for example, by generation of grain boundaries) is also possible [19]. The study of defects away from an inherent solid-fluid transition, deep in the solid phase, near a solid-solid critical point, is an opportunity to test predictions of dislocation melting theory [16].

As pointed out by Bladon and Frenkel [2], an intervening hexatic phase (the product of the first stage in the two-stage melting scenario) is likely near a two-dimensional isostructural critical point. Chen *et al.*, studying an isothermal, isobaric Lennard-Jones system, point out the large system sizes required in searching for a metastable hexatic phase [20]. Nevertheless, simulation measurements of elastic constants by Bladon and Frenkel [2] show that a dislocation instability (presumably leading to a hexatic phase) *must* develop in the vicinity of a solid-solid critical point. Since the compressibility diverges near the critical point in Fig. 1, the effective bulk modulus must soften [2]. This softening of the bulk modulus promotes dislocation unbinding, which signals the solid-hexatic transition. In this paper, we explore these ideas using a simple physical model and determine how the existence of a solid-solid critical point may induce a nearby hexatic phase. The effects of elastic degrees of freedom on the Ising critical properties in the *absence* of dislocations are also considered.

Finally, even though most simulations exhibiting a solid-solid phase transition rely on a very-short-ranged attractive potential, longer-ranged soft potentials may also show similar behavior. For example, the three-dimensional solid-solid transition in dense Cs and Ce [21] may be pressure induced [1,22]. Two-dimensional realizations such as confined colloids [8] and colloids [9] or C_{60} particles [23] at air-liquid interfaces also possess complicated short- and long-ranged interactions. However, the *two-dimensional* melting outlined relies only on a solid-solid critical point and is not sensitive to the microscopic mechanism of particle interactions.

In Sec. II we introduce two free-energy functionals including both elastic degrees of freedom and the Ising-like order parameter describing the isostructural solid-solid phase transition. Elastic deformations and the Ising order parameter are coupled via an interaction energy. We also briefly discuss symmetrically confined colloidal crystals in 2D with attractive wall potentials. If the wall potential leads to an Ising-like symmetry breaking, such that the crystal tends to be near one wall or the other, another type of isostructural critical point becomes possible.

Section III discusses the simplest model in the absence of defects. Above the critical point, the Ising degrees of freedom renormalize the elastic coefficients yielding an effective bulk modulus. Thermal fluctuations in the (single-valued) strains renormalize the critical temperature of the Ising degrees of freedom. We show that the critical temperature renormalization is different for the uniform and finite wave-vector modes in a manner such that the Ising critical point acquires *mean-field* behavior. The uniform, zero-wave-vector strains induce an infinite-ranged interaction that ensures *classical* critical exponents in this two-dimensional system.

In Sec. IV the strains and Ising order parameter in the presence of a single dislocation are studied by solving the extremal (Euler) equations. The strain field configurations are asymptotically identical to those of an uncoupled model except they are functions of effective elastic coefficients. The related Ising order parameter near the dislocation is also determined. An energy-entropy argument for an isolated dislocation leads to the melting criterion simulated by Bladon and Frenkel [2]. Qualitative phase diagrams containing solid and hexatic phases are derived based on this criterion.

The free energy of the full interacting model is expressed in terms of a collection of *many* dislocations in Sec. V. Renormalization-group flows for the parameters in the presence of a few dislocations are also derived. Dislocation-renormalized elastic moduli yield a melting criterion agreeing with simple energy-entropy considerations. The critical exponents of the crystal-hexatic transition are the same as for conventional dislocation-mediated melting [24,25].

Section VI explores transitions of the *hexatic* phase induced by the critical point. A modulated hexatic phase is possible very near the critical point. If there are no modulated hexatic instabilities, the coupling of the Ising order parameter to the hexatic bond angle field leaves the nontrivial Onsager-like critical behavior of the 2D critical point intact.

II. FREE-ENERGY MODELS

In this section we describe the free-energy functional for the physics near an isostructural critical point in terms of the elastic strain fields, an Ising-like structural order parameter, and an interaction between these degrees of freedom. Dislocations, leading to multiple-valued displacement fields will only be considered in detail in later sections.

A first-order transition in a scalar quantity such as density near a critical point can be described by an Ising model. Symmetries dictate the form of possible coupling terms. In the continuum representation, the "Landau-Ginzburg-Wilson" expression for the free energy takes the form [26]

$$\mathcal{H}_I \equiv \frac{F_I}{k_B T} = \int d^2x \left(\frac{1}{2}|\nabla\varphi|^2 + \frac{r}{2}\varphi^2 + \frac{u}{4!}\varphi^4 - h\varphi + \cdots \right), \tag{2.1}$$

where for a first-order liquid-gas transition or isostructural solid-solid transition φ is defined as the density deviation from the critical density $\varphi = \rho - \rho_c$. Near criticality, u is approximately independent of T and $r \simeq a_2(T - T_c)/T_c$. The linear term proportional to h represents a chemical potential and allows us to study the transitions at densities away from the critical isochore. Positive h favors $\varphi > 0$ (i.e., the dense phase S_2

in Fig. 1) while $h < 0$ favors $\varphi < 0$ (the dilute solid phase S_1 in Fig. 1). A potential third-order coupling ($w\varphi^3$, say) in Eq. (2.1) can be eliminated by a shift in φ.

In addition to an Ising order parameter describing the phase separation, a property of solid phases is their resistance to deformations. The elastic deformation energy is [27]

$$\mathcal{H}_{\rm el} \equiv \frac{F_{\rm el}}{k_B T} = \frac{1}{2}\int d^2x \, \left(2\mu e_{ij}^2 + \lambda e_{ii}^2\right), \tag{2.2}$$

where $e_{ij} = \frac{1}{2}(\partial_i u_j + \partial_j u_i)$ is the symmetric strain tensor and μ and λ are the Lamé coefficients defined as the microscopic Lamé coefficients divided by $k_B T$. Equation (2.2) is valid for two-dimensional triangular crystals undergoing small strains.

The free energy (2.2) in general contains both smoothly varying single-valued strains as well as singular contributions from pointlike defects such as dislocations. When a solid is thermally excited, defect complexions must be explicitly included in the statistical weight $e^{-\mathcal{H}_{\rm el}}$, as well as in a coupling term, such as Eq. (2.3) below. As discussed in Secs. IV and V, dislocations can be incorporated by considering the strains as comprised of a smooth "phonon" component u_{ij} and a singular part w_{ij}, due to the presence of defects, so that $e_{ij} = u_{ij} + w_{ij}$.

We now consider the coupling between the order parameter φ and the strain. Since the model is isotropic, symmetry requires that to leading order, only the dilatation $e_{\ell\ell}$ couples to the phase variable. The lowest-order interaction term for a phase separating system is

$$\mathcal{H}_{\rm int} = g\int d^2x \, \varphi \, e_{\ell\ell}. \tag{2.3}$$

We assume $g > 0$ so that a lattice compression ($e_{\ell\ell} < 0$) will bias the system toward $\varphi > 0$, i.e., toward the *denser* isostructural solid S_2 in Fig. 1. Related couplings between an elastic strain field and an auxiliary field have been studied in the context of compressible statistical spin models [28,29], quenched random impurities [30,31], and vacancy–interstitial defects in crystals.

For compressible magnets with an Ising-like order parameter, the relevant interaction energy is [28,29]

$$\mathcal{H}_{\rm int} = g'\int d^2x \, \varphi^2 \, e_{\ell\ell}. \tag{2.4}$$

A model of this kind would be appropriate for colloidal crystals symmetrically confined between glass plates with attractive wall potentials of the kind shown in Fig. 2. Such a double wall potential can induce (for the appropriate pair potentials between the colloidal particles) an Ising-like isostructural critical point inside the two-dimensional crystalline phase. Below the Ising phase transition, the crystal prefers to sit closer to one wall or the other. If $\varphi(\vec{x})$ represents the deviation of the local particle position from the midplane, we can use Eq. (2.1) (with $h = 0$) to represent the Ising degrees of freedom and Eq. (2.2) to model the elastic ones. The symmetrical confinement (we neglect gravity) ensures that a coupling of the form (2.3) is impossible, so we are left with (2.4).

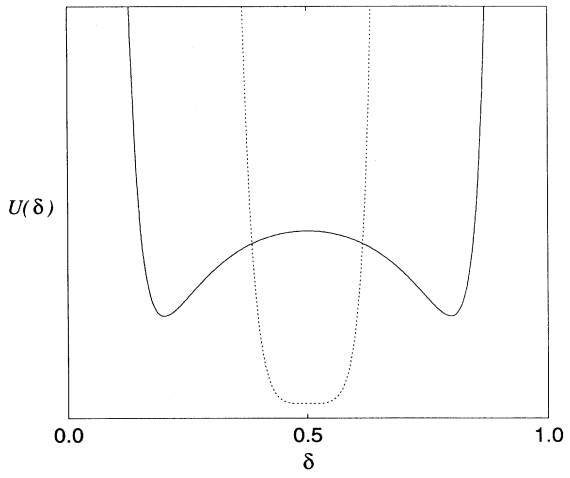

FIG. 2. Interaction potential $U(\delta)$ between particles and flat confining walls. The distance δ along the ordinate measures the distance away from the midplane $\delta = 0.5$ between the walls. When the plates are closely spaced $U(\delta)$ is given by the dashed curve corresponding to an Ising free energy above critical temperature. Increasing the plate gap lowers the temperature of the Ising-like free energy (solid curve).

As discussed, for example, by Bergman and Halperin [28], this coupling changes the critical exponents of the Ising-like transition in the *absence* of dislocations provided the specific-heat exponent α of the pure Ising system is positive. Because $\alpha = 0$ for the 2D Ising model, there is at most a very slow marginal crossover away from pure Ising-like behavior for these symmetrically confined crystals. The coupling g' induces a specific-heat-like singularity in the inverse elastic bulk modulus $\bar{B}^{-1}$ near the transition. The renormalized inverse bulk modulus can be defined as

$$\begin{aligned}\frac{1}{\bar{B}} &= \frac{1}{A}\langle U_{ii}U_{jj}\rangle \\ &= \frac{1}{B} + \frac{g'^2}{B^2}\frac{1}{A}\int d^2x \, d^2x' \langle \varphi^2(\vec{x})\varphi^2(\vec{x}')\rangle \\ &\simeq \frac{1}{B} + a_2\frac{g'^2}{B^2}\left(\frac{T - T_c}{T_c}\right)^{-\alpha},\end{aligned} \tag{2.5}$$

where $U_{ii} = \int d^2x u_{ii}(\vec{x})$, A is the system area, and $B \equiv \mu + \lambda$. If the specific heat diverges, $\bar{B} = 0$, the energy of one isolated dislocation will become small, and we again expect dislocation-mediated melting close to the critical point, similar to the argument in Ref. [2]. However, this specific-heat singularity is much weaker than the singularity that induces melting for an asymmetrical model, so a hexatic phase may be difficult to observe experimentally.

In the remainder of this paper we consider the linear coupling (2.3), where the effects are expected to be more dramatic. The total free energy is thus

$$\mathcal{H} = \int d^2x \left[\mu e_{ij}^2 + \frac{\lambda}{2} e_{ii}^2\right] + g \int d^2x e_{\ell\ell}\varphi$$

$$+ \int d^2x \left[\frac{1}{2}|\nabla\varphi|^2 + \frac{r}{2}\varphi^2 + \frac{u}{4!}\varphi^4 - h\varphi + \cdots\right]. \quad (2.6)$$

Figure 3 shows schematically the coexistence of two different density phases of lattice constant a_+ and a_-. Under a uniform area change, the system responds by undergoing both pure dilatational elastic deformations in each of the phases as well as interconversion between local regions of phase S_1 or S_2. The relative partition between these two responses is governed by g. In the Appendix we discuss the stability constraints on the coupling constants determined from Eq. (2.6) expanded to quadratic order.

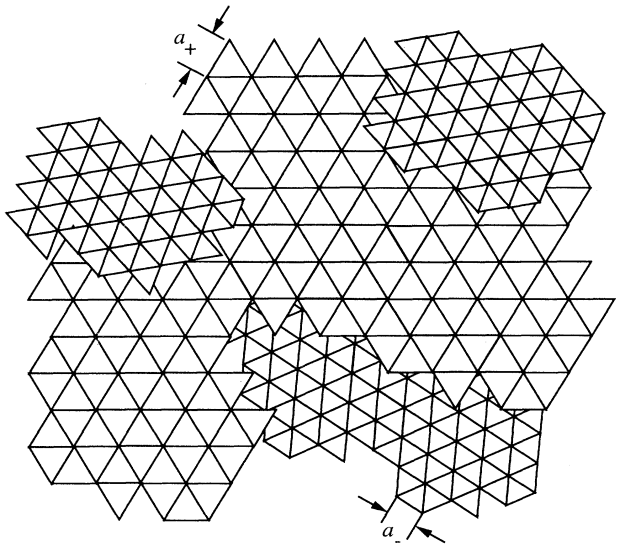

FIG. 3. Coexistence of two isostructural solid phases S_1 and S_2 with lattice constants a_+ and a_-, respectively.

III. DEFECT-FREE LIMIT

In this section we study the interplay between the strain and Ising fields in the absence of defects. The strain fields u_{ij} are single valued and can be thermally averaged out in the quadratic theory. We assume free boundary conditions in the (x_1, x_2) plane and write the Fourier transformed strain in terms of uniform bulk distortions and finite wave-vector modes [32]

$$u_{ij}(\vec{x}) = u_{ij}^{(0)} + \frac{1}{2A}\sum_{\vec{q}\neq\vec{0}} i[q_i u_j(\vec{q}) + q_j u_i(\vec{q})]e^{i\vec{q}\cdot\vec{x}}. \quad (3.1)$$

In the decomposition (3.1), the uniform symmetric strains $u_{ij}^{(0)}$ must be treated separately because these require *three* degrees of freedom, in contrast to the two independent phonon modes that arise when $\vec{q} \neq \vec{0}$. A similar treatment is required in the study of the zero-wave-vector excitation in Bose-Einstein condensation.

Similar to (3.1), we decompose $\varphi(\vec{x})$ as

$$\begin{aligned}\varphi(\vec{x}) &= \varphi_0 + \sum_{\vec{q}\neq\vec{0}} \tilde{\varphi}(\vec{q}) e^{i\vec{q}\cdot\vec{x}} \\ &= \varphi_0 + \delta\varphi(\vec{x}).\end{aligned} \quad (3.2)$$

For the linear coupling model (2.3) considered here, the zero-wave-vector strain modes couple only to the zero-wave-vector Ising field φ_0. After integrating out these uniform bulk strains, we find an effective energy for φ_0. Averaging over the fluctuating crystal displacements $[\vec{u}(\vec{q}), \vec{q} \neq \vec{0}]$, however, gives a different effective energy for the nonzero-wave-vector Ising fields $\delta\varphi(\vec{x})$. The final result including the quartic coupling is

$$\mathcal{H}_{\rm eff}[\varphi] = A\left[\left(\frac{r}{2} - \frac{g^2}{2B}\right)\varphi_0^2 + \frac{u}{4!}\varphi_0^4 - h\varphi_0\right] + \frac{1}{2}\int d^2x \left[|\vec{\nabla}\varphi|^2 + \left(r - \frac{g^2}{(\mu+B)} + \frac{u}{2}\varphi_0^2\right)\delta\varphi^2(\vec{x})\right]$$
$$+ \frac{u}{6A^3}\varphi_0 \sum_{\vec{q}_1\neq\vec{0}} \sum_{\vec{q}_2\neq -\vec{0},\vec{q}_1} \varphi(\vec{q}_1)\varphi(\vec{q}_2)\varphi(-\vec{q}_1 - \vec{q}_2) + \frac{u}{4!}\int d^2x \delta\varphi^4(\vec{x}) + \cdots, \quad (3.3)$$

where $\delta\varphi(\vec{x})$ contains only finite-wave-vector perturbations of the Ising order parameter about its uniform value φ_0.

The $\vec{q} = \vec{0}$ strains ($u_{ij}^{(0)}$) renormalize the φ_0 modes differently than the finite-wave-vector phonons $[\vec{u}(\vec{q})]$ renormalize the $\varphi(\vec{q} \neq \vec{0})$ modes. The critical temperature of φ_0 is shifted according to $T^* \approx T_c(1 + g^2/a_2 B)$. The mass or quadratic coefficient of the φ_0 field (denoted $\bar{r}_0$) will, upon decreasing temperature, always vanish before the quadratic coupling of the finite-wave-vector modes (denoted $\bar{r}$). Thus $\bar{r}_0 < \bar{r}$, where

$$\bar{r}_0 \equiv r - \frac{g^2}{B} \quad (3.4)$$

and

$$\bar{r} \equiv r - \frac{g^2}{(\mu+B)} + \frac{u}{2}\varphi_0^2. \quad (3.5)$$

Since the $\delta\varphi(\vec{x})$ modes remain massive near $\bar{r}_0 \approx 0$, they can be integrated out in perturbation theory to give a renormalized effective potential (with no gradient term) for the remaining φ_0 degree of freedom. It is

easily checked that the ordering of φ_0 prevents the subsequent ordering of the $\delta\varphi(\vec{x})$ modes at a lower temperature within our model. We conclude that the critical behavior of a 2D Ising model interacting with strain fields according to Eq. (2.3) is described by mean-field exponents.

The physical reason for mean-field critical behavior is that the uniform strains induce an infinite-ranged interaction between the zero-wave-vector Ising degrees of freedom. To see this, note that the quadratic contributions to Eq. (3.3) may be combined to give

$$\mathcal{H}_{\rm eff}^{(2)} = \frac{1}{2}\int d^2x \left[|\nabla\varphi(\vec{x})|^2 + \left(r - \frac{g^2}{\mu+B}\right)\varphi^2(\vec{x})\right] - \frac{\mu g^2}{A(\mu+B)B}\int d^2x \int d^2x' \varphi(\vec{x})\varphi(\vec{x}'). \quad (3.6)$$

The first term is the usual continuum representation of a short-ranged interaction, but the second has infinite range, induced by the strain coupling.

It is also instructive to consider elastic constants as renormalized by fluctuations of the Ising variable. It is easy to show that integrating over the slowly varying φ degrees of freedom leads to an effective Lamé coefficient

$$\bar{\lambda} = \lambda - g^2/r', \quad (3.7)$$

where

$$r' = r + \frac{u}{2}\varphi_0^2. \quad (3.8)$$

Consider the behavior of the effective elastic constant $\bar{\lambda}$ near the (mean-field) critical temperature T^* discussed above. Recall that $\bar{r}_0(T^*) = 0$ and let us assume for simplicity that $h = 0$ and $T \le T^*$. Since $r' = r$ in this case, we have $r'(T^*) = r(T^*) = g^2/B = g^2/(\mu+\lambda)$. It follows that

$$\bar{\lambda}(T^*) = -\mu \quad (3.9)$$

so that the effective bulk modulus

$$\bar{B}(T) = \mu + \bar{\lambda} \quad (3.10)$$

vanishes as $T \to T^*$. This vanishing of the effective bulk modulus is expected quite generally, since $\bar{B}$ is related to the Ising fluctuations in our model by an equation similar to (2.5), namely,

$$\frac{1}{\bar{B}} = \frac{1}{A}\langle U_{ii}U_{jj}\rangle = \frac{1}{B} + \frac{g^2}{B^2}\frac{1}{A}\int d^2x \int d^2x' \langle\varphi(\vec{x})\varphi(\vec{x}')\rangle. \quad (3.11)$$

The strongly divergent mean-field Ising fluctuations $\frac{1}{A}\int d^2x \int d^2x' \langle\varphi(\vec{x})\varphi(\vec{x}')\rangle \sim (T-T^*)^{-1}$ ensure that $\bar{B}$ vanishes. The reduction in λ implied by (3.7) corresponds to a lattice softening, suggesting that dislocations can more easily form.

The conditions of stability are different for zero-wave-vector and finite-wave-vector instabilities consistent with the renormalized "masses" for $\vec{q} = \vec{0}$ and $\vec{q} \neq \vec{0}$ fluctuations $\bar{r}_0$ and $\bar{r}$, respectively. Linear stability analysis of the defect-free model is given in the Appendix.

IV. ISOLATED DISLOCATION

In this section we determine the behavior of φ and the strains with a single dislocation at the origin. We also calculate the free energy of this dislocation and apply an energy-entropy balance to predict when dislocations are favored. The dislocation contribution to the field configurations is found by solving the extremal equations developed below.

We first write the total strain as

$$e_{ij} = u_{ij}^{(0)} + w_{ij}, \quad (4.1)$$

where $u_{ij}^{(0)}$ is the $\vec{q} = \vec{0}$ part and w_{ij} are the singular strains due to the dislocation. After minimizing with respect to $u_{ij}^{(0)}$ and expanding $\varphi(\vec{x})$ about a uniform value $\varphi_0 + \delta\varphi(\vec{x})$, we find that the effective free energy becomes (to quadratic order in $\delta\varphi$)

$$\mathcal{H}_{\rm eff}[\varphi, w_{ij}] = A\left[\frac{\bar{r}_0}{2}\varphi_0^2 + \frac{u}{4!}\varphi_0^4 - h\varphi_0\right] + \int d^2x \left[\mu w_{ij}^2 + \frac{\lambda}{2}w_{ii}^2 + g\delta\varphi w_{ii} + \frac{1}{2}|\nabla\delta\varphi|^2 + \frac{r'}{2}\delta\varphi^2 + O(\delta\varphi^3)\right], \quad (4.2)$$

where $\bar{r}_0$ is given by Eq. (3.4) and r' is given by Eq. (3.8). Near a dislocation φ distorts from φ_0. We will assume that $\varphi(\vec{x} \to \infty) \to \varphi_0$, where φ_0 is one of possibly two uniform minima. This *ansatz* is appropriate in the presence of a single dislocation, since domain walls connecting regions with $\varphi = \varphi_0$ and $-\varphi_0$ would cost an additional gradient energy scaling as the system size.

After minimizing (4.2) with respect to φ_0, $\delta\varphi(\vec{x})$, and $\vec{u}$, the displacement caused by the dislocation, we obtain

$$\bar{r}_0\varphi_0 + \frac{u}{6}\varphi_0^3 - h + \frac{u}{2}\varphi_0 \int d^2x \delta\varphi^2(\vec{x}) = 0, \quad (4.3)$$

$$-\nabla^2\delta\varphi + r'\delta\varphi + g w_{ii} + O\left(\delta\varphi^2\right) = 0, \quad (4.4)$$

and

$$\mu\nabla^2\vec{u} + (\mu+\lambda)\vec{\nabla}(\vec{\nabla}\cdot\vec{u}) + g\vec{\nabla}\delta\varphi = -\mu\hat{z}\times\vec{b}\delta(\vec{x}), \quad (4.5)$$

where $\vec{u}$ in (4.5) is understood to be the lattice displacement due to the dislocation $w_{ij} = \frac{1}{2}(\partial_i u_j + \partial_j u_i)$. These strains that satisfy the extremal equations guarantee vanishing of cross terms between u_{ij} and w_{ij} in (4.2). We follow the treatment in Ref. [27] and write the displacement vector as $\vec{u} = \vec{u}_0 + \vec{u}'$, where $\vec{u}_0$ assumes the Burgers vector when integrated around a dislocation, i.e., $\nabla^2\vec{u}_0 = -\hat{z}\times\vec{b}\delta(\vec{x})$. Note also that $\vec{\nabla}\cdot\vec{u}_0 = 0$. By taking the divergence of (4.5) and substituting in the expression

for $(\vec{\nabla}\cdot\vec{u})$ from (4.4), we obtain a closed equation for $\delta\varphi(\vec{x})$,

$$-\nabla^4\delta\varphi+\left(r'-\frac{g^2}{\mu+B}\right)\nabla^2\delta\varphi=\frac{2\mu g}{\mu+B}\vec{\nabla}\cdot[\hat{z}\times\vec{b}\delta(\vec{x})]. \tag{4.6}$$

Note that we have retained the gradient contribution to the energy in Eq. (4.4). The value of φ_0 must be determined self-consistently; however, for small $\delta\varphi(\vec{x})$, the correction to $\bar{r}_0$ in (4.3) is small and φ_0 can be approximated by the solution to

$$\bar{r}_0\varphi_0+\frac{u}{6}\varphi_0^3-h\approx 0. \tag{4.7}$$

Having determined the boundary conditions for a single dislocation at the origin, we can solve for a small deviation of the Ising order parameter $\delta\varphi(\vec{x})$. With $\vec{x}=\{x_1,x_2\}$ and $\vec{b}=b\hat{e}_1$, where $\hat{e}_1$ is a unit vector in the x_1 direction,

$$\delta\varphi(\vec{x})\simeq\frac{\mu g b}{\pi\kappa^2(\mu+B)}\frac{x_2}{|\vec{x}|^2}\left[1-\sqrt{\frac{\pi}{2\kappa|\vec{x}|}}e^{-\kappa|\vec{x}|}\right], \tag{4.8}$$

where

$$\begin{aligned}\kappa^2&=\bar{r}\\&=r'-\frac{g^2}{\mu+B}.\end{aligned} \tag{4.9}$$

A plot of $\delta\varphi(\vec{x})$ is shown in Fig. 4. The peaks and valleys ($x_2>0$ and $x_1<0$, respectively) correspond to a missing or extra row of particles. We also calculate the dilatation [Eq. (4.4)]

$$\vec{\nabla}\cdot\vec{u}=w_{ii}\simeq-\frac{\mu b r'}{\pi\kappa^2(\mu+B)}\frac{x_2}{|\vec{x}|^2}\left[1-O\left(|\vec{x}|^3e^{-\kappa|\vec{x}|}\right)\right], \tag{4.10}$$

which is asymptotically inversely proportional to $\delta\varphi$. The total displacements can be found from

$$\mu\nabla^2\vec{u}'=-(\mu+\lambda)\vec{\nabla}w_{ii}-g\vec{\nabla}\delta\varphi-2\mu b\delta(\vec{x})\hat{e}_2. \tag{4.11}$$

We note that $\partial w_{ii}/\partial x_2$ and $\partial\delta\varphi/\partial x_2$ behave as δ functions at the origin and find the total displacements around a dislocation

$$\begin{aligned}u_1&=\frac{b}{2\pi}\left[\tan^{-1}\left(\frac{x_2}{x_1}\right)+\frac{Br'-g^2}{\kappa^2(\mu+B)}\frac{x_1x_2}{|\vec{x}|^2}\right]+O(e^{-\kappa|\vec{x}|}),\\u_2&=-\frac{b}{2\pi}\left[\frac{\mu r'}{\kappa^2(\mu+B)}\ln|\vec{x}|+\frac{Br'-g^2}{\kappa^2(\mu+B)}\frac{x_1^2}{|\vec{x}|^2}\right]\\&\quad+O(e^{-\kappa|\vec{x}|}).\end{aligned} \tag{4.12}$$

These displacements are asymptotically identical to those of standard elasticity theory [27], except with λ replaced by $\bar{\lambda}$.

Evaluating (4.2) to quadratic order using asymptotic expressions for $\vec{u}$ and $\delta\varphi$ gives the total energy of a single dislocation of strength b,

$$\mathcal{H}_{\rm eff}=\frac{\bar{K}b^2}{8\pi}\ln\left(\frac{R}{a}\right)+c(a), \tag{4.13}$$

where R is the linear sample dimension and $c(a)$ is a function of the dislocation core size a. The most singular part of the energy (4.13) has the same form as the standard result, except with effects of the coupling $\mathcal{H}_{\rm int}$ contained in an effective Young modulus

$$\bar{K}=\frac{4\mu(\mu+\bar{\lambda})}{2\mu+\bar{\lambda}}, \tag{4.14}$$

where the effective Lamé coefficient for a dislocation is given by

$$\bar{\lambda}=\lambda-\frac{g^2}{r'}, \tag{4.15}$$

consistent with Eq. (3.7). As discussed in Sec. III, this reduction of λ causes the effective bulk modulus $\bar{B}=\mu+\bar{\lambda}$ to vanish near the isostructural critical point.

The total free energy of a dislocation G_1 also includes entropy describing configurations associated with the $(R/a)^2$ possible positions the dislocation can occupy. Hence

$$G_1/k_BT=\mathcal{H}_{\rm eff}-2\ln(R/a). \tag{4.16}$$

The temperature above which the entropy favors dislocation formation is given by $G_1/k_BT\approx 0$ or

$$\bar{K}\approx 16\pi. \tag{4.17}$$

This criterion, modified from the Kosterlitz-Thouless criterion of the decoupled theory [$4\mu B/(\mu+B)\approx 16\pi$] [33], determines the phase diagram. The onset of dislocation melting occurs when $K>\bar{K}$, where

$$\begin{aligned}\bar{K}&=\frac{4\mu\left[Br'-g^2\right]}{(\mu+B)r'-g^2}\\&=\frac{4\mu(\mu+\bar{\lambda})}{2\mu+\bar{\lambda}}=16\pi.\end{aligned} \tag{4.18}$$

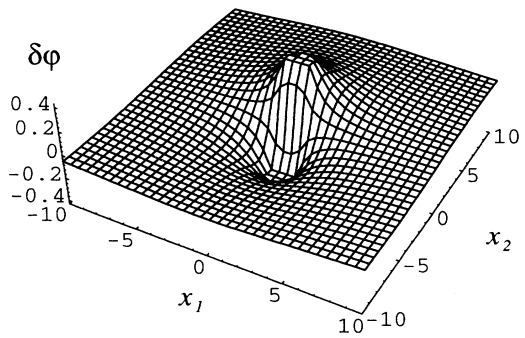

FIG. 4. Solution $\delta\varphi$ for $\vec{b}=-b\hat{e}_1$ plotted in dimensionless units of $\mu g b/\pi\kappa^2(\mu+B)$. Distances x_i have units of κ^{-1}. Note that φ diverges at the dislocation and a cutoff must be imposed before $\delta\varphi$ gets too large; however, unlike the phonon displacement field $\vec{u}$, $\delta\varphi(\vec{x})$ is single valued.

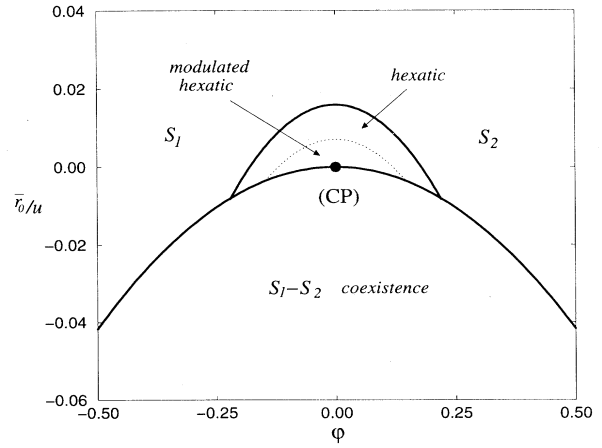

FIG. 5. Phase diagram near the critical point of an isostructural solid-solid transition projected on the dimensionless $\bar{r}_0/u$-φ plane. For $\mu = \lambda = 10\pi$, a lobe of hexatic phase is induced near the critical point. The solid hexatic-solid boundary corresponds to $g^2/u = 2$. The hexatic region becomes smaller for smaller g^2/u. A modulated hexatic phase, evaluated using $v^2/K_B = 1/45\pi$, lies within the thin dotted line. The S_1-S_2 coexistence line is approximated by mean-field theory.

This condition is equivalent to the usual Kosterlitz-Thouless criterion, with the replacement $B \to \bar{B} = B - g^2/r'$. Because $\bar{B}(T) \to 0$ as $T \to T^*$, melting is inevitable near the isostructural critical point. To obtain phase diagrams, we assume μ and B to be slowly varying functions of the order parameter φ. If we further assume for simplicity that bare elastic constants (unrenormalized by either Ising order parameter fluctuations or dislocations) satisfy $\mu(\rho_c) \approx \lambda(\rho_c)$, the original dislocation-mediated melting theory ($g = 0$) predicts dislocation unbinding when $\mu(\rho_c), \lambda(\rho_c) \approx 6\pi$. However, in the modified Kosterlitz-Thouless criterion (4.18), the effective parameters may be such that (4.18) is satisfied even when $\mu, \lambda > 6\pi$. In the $(\bar{r}_0/u, \rho - \rho_c)$ plane, the boundary of a hexatic phase near the isostructural critical point as found from (4.18) is shown in Fig. 5.

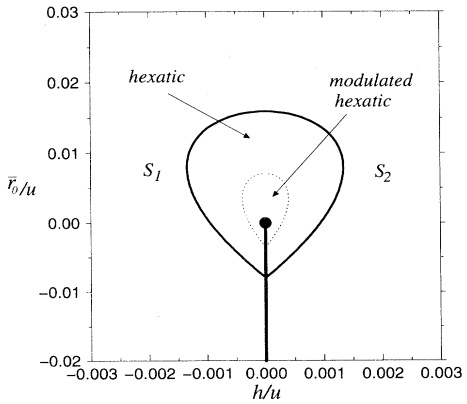

FIG. 6. Phase boundaries projected on the dimensionless $\bar{r}_0/u$-h/u plane for $\mu = \lambda = 10\pi$ and $g^2/u = 2.0$. The smaller lobe corresponding to a modulated hexatic phase is shown by the thin dotted line. A line of discontinuous transitions is represented by the dark line along the x axis and a renormalized mean-field critical point is at the origin.

We use the solution of the cubic equation (4.7) in (4.18) to obtain a quantitative picture in the h-T plane. Phase boundaries for $\mu = \lambda = 10\pi$ in the $\bar{r}_0/u$-h/u plane are plotted in Fig. 6. Phase diagrams topologically similar to those shown in Figs. 5 and 6 have been included in the study of liquid crystals [34]. More precise determination of the phase boundary would require a first-principles calculation of the unrenormalized elastic moduli μ and λ. This can be obtained for example by density-functional theory [12] or primitive cell models [1]. Our simple model, however, shows salient features of 2D melting induced by an isostructural critical point and agrees qualitatively with the simulated phase diagram of Bladon and Frenkel [2].

V. EFFECTS OF MANY DISLOCATIONS

When many dislocations are present, the possibility of more complicated structures arises. In particular, dislocations may aggregate to form grain boundaries or extended domains where φ may take on values different from φ_0, or for $\bar{r}_0 < 0$, both domains of $+\varphi_0$ and $-\varphi_0$ phases may coexist. We will assume that these complex aggregates do not form. Here we assume a dilute dislocation gas and demonstrate that the renormalization-group recursion relations for the effective parameters are unchanged from those of the uncoupled melting theory.

The stress tensor associated with $\mathcal{H} \equiv \mathcal{H}_{\rm el} + \mathcal{H}_I + \mathcal{H}_{\rm int}$ is

$$\sigma_{ij} = (\mu + \lambda) e_{\ell\ell}\delta_{ij} + 2\mu(e_{ij} - \tfrac{1}{2} e_{\ell\ell}\delta_{ij}) + 2g\varphi\,\delta_{ij}, \quad (5.1)$$

which can be inverted to give

$$e_{ij} = \frac{1}{2\mu}\sigma_{ij} - \frac{\lambda}{4\mu(\mu+\lambda)}\sigma_{\ell\ell}\delta_{ij} - \frac{g}{\mu+\lambda}\varphi\,\delta_{ij}. \quad (5.2)$$

Functional minimization with respect to the phonon displacements yields a divergence-free stress

$$\partial_i \sigma_{ij}^{(s)} = 0 \quad (5.3)$$

to which single-valued fluctuating stresses $\tilde{\sigma}_{ij}$ must be added. Since (5.3) holds away from defects, the extremal stress can be expressed in terms of a double curl [27]

$$\sigma_{ij}^{(s)} \equiv \epsilon_{im}\epsilon_{jn}\partial_m\partial_n\chi. \quad (5.4)$$

For the present problem, the stress tensor for a collection of dislocations at positions $\{\vec{x}_\alpha\}$ with the Burgers vectors $\{\vec{b}_\alpha\}$ and "Burgers charge density"

$$\vec{b}(\vec{x}) = \sum_\alpha \vec{b}_\alpha \delta(\vec{x} - \vec{x}_\alpha)$$

is given by

$$\sigma_{ij} = \sigma_{ij}^{(s)} + \tilde{\sigma}_{ij}$$
$$= -\frac{K_0}{4\pi}\epsilon_{im}\epsilon_{jn}\partial_m\partial_n \int d^2x' b_k(x')\epsilon_{kl}(x-x')_\ell \times \left[\ln\frac{|\vec{x}-\vec{x}'|}{a} + C\right] + \frac{gK_0}{\mu+\lambda}\epsilon_{im}\epsilon_{jn}\partial_n\partial_m \times \int d^2x' G(x-x')\nabla^2\varphi(x') + \tilde{\sigma}_{ij}, \quad (5.5)$$

where $\nabla^4 G(\vec{x}) = \delta(\vec{x})$ and C is a constant of order unity. The functional form of the free energy $\mathcal{H} = \frac{1}{2}\int d^2x \sigma_{ij}e_{ij} + \mathcal{H}_I$ becomes

$$\mathcal{H} = \mathcal{H}_I[\varphi] + \mathcal{H}_0[u_{ij}] + \mathcal{H}_{\rm int}[\varphi, u_{ij}] + \mathcal{H}_D[\vec{b}]\mathcal{H}_{\rm int}^{\rm sing}[\varphi,\vec{b}], \quad (5.6)$$

where u_{ij} is the smoothly varying part of the strain and

$$\mathcal{H}_D = -\frac{K_0}{8\pi}\sum_{\alpha\neq\beta}\left[\vec{b}(\vec{x}_\alpha)\cdot\vec{b}(\vec{x}_\beta)\ln\left(\frac{|\vec{x}_\alpha-\vec{x}_\beta|}{a}\right) - \frac{\vec{b}(\vec{x}_\alpha)\cdot(\vec{x}_\alpha-\vec{x}_\beta)\vec{b}(\vec{x}_\beta)\cdot(\vec{x}_\alpha-\vec{x}_\beta)}{|\vec{x}_\alpha-\vec{x}_\beta|^2}\right] + \frac{E_c}{k_BT}\sum_\alpha |\vec{b}(\vec{x}_\alpha)|^2. \quad (5.7)$$

The dislocation contribution to the strain w_{ii} may be written in terms of the Burgers vectors [33,24,30]

$$w_{ii}(\vec{x}) = -\frac{K_0}{4\pi(\mu+\lambda)}\sum_\alpha \frac{\hat{z}\cdot[\vec{b}(\vec{x}_\alpha)\times(\vec{x}-\vec{x}_\alpha)]}{|\vec{x}-\vec{x}_\alpha|^2}, \quad (5.8)$$

which leads to

$$\mathcal{H}_{\rm int}^{\rm sing}[\varphi,\vec{b}] = g\int d^2x w_{ii}\varphi = \frac{gK_0}{4\pi(\mu+\lambda)}\sum_\alpha\int d^2x\,\varphi(\vec{x}) \times\frac{\hat{z}\cdot[\vec{b}(\vec{x}_\alpha)\times(\vec{x}-\vec{x}_\alpha)]}{|\vec{x}-\vec{x}_\alpha|^2}. \quad (5.9)$$

If the fluctuations in $\delta\varphi(\vec{x})$ are now averaged out, the effective model of interacting dislocations takes the form of $\mathcal{H}_D$, except with the replacement $K_0 \to \bar{K}$, with $\bar{K}$ given by (4.18). Although we have omitted the details, these results follow from straightforward generalizations of (4.3)–(4.5). For example, (4.5) is generalized as

$$\mu\nabla^2\vec{u} + (\mu+\lambda)\vec{\nabla}(\vec{\nabla}\cdot\vec{u}) + g\vec{\nabla}\varphi = \mu\sum_\alpha \hat{z}\times\vec{b}_\alpha\delta(\vec{x}-\vec{x}_\alpha). \quad (5.10)$$

The energy (5.6) can be analyzed by rescaling dislocation core sizes and distances in a way similar to that discussed in [25]. Although recursion relations for g and r as well as the elastic coefficients can be found this way, it is simpler to construct recursion relations in terms of the effective coupling $\bar{K}$. These recursion relations are [24,25]

$$\frac{dy(\ell)}{d\ell} = \left[2 - \frac{\bar{K}(\ell)}{8\pi}\right]y(\ell) + 2\pi y^2(\ell)e^{\bar{K}(\ell)/16\pi}I_0(\bar{K}(\ell)/8\pi) + O(y^3(\ell)), \quad (5.11)$$

$$\frac{d\bar{K}^{-1}(\ell)}{d\ell} = \frac{3\pi}{2}y^2(\ell)e^{\bar{K}(\ell)/8\pi}\left[I_0(\bar{K}(\ell)/8\pi) - \frac{1}{2}I_1(\bar{K}(\ell)/8\pi)\right] + O(y^3(\ell)), \quad (5.12)$$

where $\bar{K}(\ell)$ is defined by (4.18), $y(\ell)$ is the dislocation fugacity $y \simeq e^{-E_c/k_BT}$, and I_0 and I_1 are modified Bessel functions. $\bar{K}(\ell)$ and $y(\ell)$ are the usual scale-dependent renormalization-group coupling constants. The $O(y^2)$ term on the right-hand side of (5.11) is found by considering three dislocation configurations [24]. Flows of the parameters, as one considers increasing length scales ℓ, for which $y \to 0$, indicate states with proliferated dislocations, or a hexatic phase. A melting criterion identical to the modified Kosterlitz-Thouless criterion [Eq. (4.18)] arises from an analysis of (5.11). Moreover, we conclude that the critical properties of standard dislocation melting theory [24], such as an essential singularity in the specific-heat, and a divergence of the translational correlation length of the form $\xi_+(T) \sim \exp(\text{const}/|T-T_m|^{0.369\,63})$ are unchanged from the result of the usual dislocation-mediated theory.

VI. HEXATIC MELTING AND DISCLINATION UNBINDING

In this section we examine the stability of the critical-point-induced hexatic phase. Within the hexatic phase, when many dislocations are unbound, the free energy is described by slow spatial variations in the bond angle field [35,24]. The lowest-order symmetry-allowed coupling between the bond angle θ and Ising order parameter has the form $v\vec{\nabla}\theta\cdot\vec{\nabla}\varphi$ and the total free energy is

$$\mathcal{H}_{\rm hex} = \frac{K_A}{2}\int d^2x\,|\vec{\nabla}\theta|^2 + v\int d^2x\,\vec{\nabla}\theta\cdot\vec{\nabla}\varphi + \mathcal{H}_I[\varphi], \quad (6.1)$$

where K_A is the hexatic stiffness constant; $K_A(T) \to \infty$ as the freezing transition is approached from the hexatic phase [24]. We now consider the behavior of the bond angle and density order parameter in the presence of disclinations. The hexatic phase predicted from the standard dislocation melting theory will melt into an isotropic fluid phase upon further increase in temperature. Proliferating disclinations cause this first-order transition.

For our model (6.1), we find that the interactions between disclinations and φ fields decouple. To see this, we first write the extremal equations derived from (6.1),

$$K_A\nabla^2\theta + v\nabla^2\varphi = 0, \quad (6.2)$$

$$-\nabla^2\varphi + r\varphi + \frac{u}{6}\varphi^3 - h - v\nabla^2\theta = 0. \quad (6.3)$$

Note that Eq. (6.2) allows us to define a conjugate bond angle field

$$\epsilon_{ij}\partial_j\tilde{\theta} \equiv \partial_i\theta + \frac{v}{K_A}\partial_i\varphi. \tag{6.4}$$

The density order parameter is assumed to be single valued; however, the bond angle θ obeys the noncommutivity relation implied by a set of disclinations located at positions $\{\vec{x}_\alpha\}$,

$$\epsilon_{ij}\partial_i\partial_j\theta = m(\vec{x}) = \frac{\pi}{3}\sum_\alpha s_\alpha\delta(\vec{x}-\vec{x}_\alpha). \tag{6.5}$$

The strength of the αth singularity is measured by the charge $s_\alpha = \pm 1$. Thus we find

$$\partial_i\theta(\vec{x}) = \epsilon_{ij}\int d^2x'\, m(\vec{x}')\partial_j G(\vec{x}-\vec{x}') - \frac{v}{K_A}\partial_i\varphi(\vec{x}). \tag{6.6}$$

Using Eq. (6.6), we find that the terms coupling the disclination positions to $\varphi(\vec{x})$ vanish and

$$\begin{aligned}\mathcal{H}_V = {} & \frac{-\pi K_A}{36}\sum_{\vec{x}\neq\vec{x}'} s(\vec{x})s(\vec{x}')\ln\frac{|\vec{x}-\vec{x}'|}{a} \\ & + \frac{E_c}{k_BT}\sum_{\vec{x}} s^2(\vec{x}) + \frac{K_A}{2}\int d^2x\,|\vec{\nabla}\tilde{\theta}|^2 \\ & + v\int d^2x\,\vec{\nabla}\tilde{\theta}\cdot\vec{\nabla}\varphi \\ & + \int d^2x\,\left[\frac{1}{2}|\vec{\nabla}\varphi|^2 + \frac{r}{2}\varphi^2 + \frac{u}{4!}\varphi^4 - h\varphi\right],\end{aligned} \tag{6.7}$$

where $\tilde{\theta}$ represents the smoothly varying part of the bond angle field. In addition to a possible disclination unbinding transition, a finite-wave-vector instability may develop when higher-order terms in $\vec{\nabla}\varphi$ are included in (6.7). If we expand (6.7) to quadratic order about the minimum of φ and average over the smooth density fluctuations, we find

$$\begin{aligned}\mathcal{H}_V = {} & \frac{-\pi K_A}{36}\sum_{\vec{x}\neq\vec{x}'} s(\vec{x})s(\vec{x}')\ln\frac{|\vec{x}-\vec{x}'|}{a} \\ & + \frac{E_c}{k_BT}\sum_{\vec{x}} s^2(\vec{x}) + \frac{K_A}{2}\int d^2x\,|\vec{\nabla}\tilde{\theta}|^2 \\ & + \frac{\bar{K}_B}{2}\int d^2x\,|\nabla^2\tilde{\theta}|^2 + \frac{K_C}{2}\int d^2x\,|\vec{\nabla}\nabla^2\tilde{\theta}|^2,\end{aligned} \tag{6.8}$$

where we have added higher-order terms $\frac{1}{2}K_B|\vec{\nabla}^2\tilde{\theta}|^2$ and $\frac{1}{2}K_C|\vec{\nabla}\nabla^2\tilde{\theta}|^2$ to Eq. (6.7) and defined

$$\bar{K}_B \equiv K_B - \frac{v^2}{r + \frac{u}{2}\varphi_0^2}. \tag{6.9}$$

Either expression (6.7) or (6.8) shows that the interaction energy in (6.1) decouples from the disclination configurations and only modifies the effective stiffness of the φ or θ_0 fields.

Note from Eq. (6.9) that $\bar{K}_B$ becomes negative near the isostructural critical point at $r = \varphi_0 = 0$. For $\bar{K}_B < 0$, a finite-wave-vector instability in bond angle (along with density) occurs at

$$q^* = \pm\frac{|\bar{K}_B|}{\sqrt{3K_C}}\sqrt{1+\sqrt{1-3K_AK_C/\bar{K}_B}}, \tag{6.10}$$

provided that $1/q^*$ is larger than the lattice or disclination cutoff size. The thin dotted lines in Figs. 5 and 6 show the possible modulated hexatic phase. Near the critical point, disclination unbinding and melting directly to an isotropic fluid is also possible.

In principle, the solid could melt directly into a modulated hexatic phase via a first-order transition. Curves delineating possible hexatic-modulated hexatic and solid-modulated hexatic phase boundaries are shown in Figs. 5 and 6.

Provided that the gradient coefficient in (6.7) remains positive, the critical point retains nonclassical 2D Ising critical behavior. Coupling to bond angle degrees of freedom does not induce the long-ranged elastic interactions that lead to the mean-field critical behavior discussed in Sec. III.

ACKNOWLEDGMENTS

We are grateful to D. Frenkel for a copy of [2] prior to publication and to B. I. Halperin, C. A. Murray, and J. Toner for helpful discussions. This work was supported by the National Science Foundation, primarily through the Harvard Materials Research Science and Engineering Center via Grant No. DMR-9400396 and in part through Grant No. DMR-9417047.

APPENDIX: STABILITY ANALYSIS

Bounds on the elastic parameters in Eq. (5.6) follow from a stability analysis in the absence of dislocations. We set $h = 0$ for simplicity. Two cases must be treated separately. First, we analyze stability with respect to the two components of the displacements $\vec{u}$. Then, stability with respect to the three components of zero-wave-vector strains is checked.

We first write the Fourier-transformed Hamiltonian after decomposing the strains into uniform bulk distortions and finite-wave-vector modes as in Ref. [32]. In the decomposition (3.1), the uniform symmetric strains $u_{ij}^{(0)}$ must be treated separately because these require *three* degrees of freedom, in contrast to the two independent modes when $\vec{q}\neq\vec{0}$. First consider the finite-$\vec{q}$ contribution to the quadratic part of $\mathcal{H}$

$$\begin{aligned}\mathcal{H}^{(2)}_{\vec{q}\neq\vec{0}} = {} & \frac{1}{2}\sum_{\vec{q}\neq\vec{0}} u_iD_{ij}(\vec{q})u_j + \frac{1}{2}\sum_{\vec{q}\neq\vec{0}}(q^2+r)|\varphi(\vec{q})|^2 \\ & - g\sum_{\vec{q}\neq\vec{0}} iq_iu_i\varphi(\vec{q}),\end{aligned} \tag{A1}$$

where the phonon dynamical matrix is

$$D_{ij}(\vec{q}) = \mu q^2 \delta_{ij} + (\mu + \lambda) q_i q_j. \tag{A2}$$

The eigenvalues of the quadratic form (A1) are given by

$$\begin{aligned}\Lambda_0 &= \mu q^2, \\ \Lambda_\pm &= \frac{(2\mu+\lambda)q^2 + r + q^2}{2} \\ &\quad \pm \frac{1}{2}\{[(2\mu+\lambda)q^2 + r + q^2]^2 \\ &\quad -4(2\mu+\lambda)q^2(r+q^2) + g^2 q^2\}^{1/2}.\end{aligned} \tag{A3}$$

The onset of instability occurs when an eigenvalue vanishes. Thus the system is stable against long-wavelength ($q \to 0$) modes when $\mu > 0$ and $r > g^2/(2\mu + \lambda)$.

For uniform distortions, the quadratic terms in the energy can be written in terms of the three independent components of the strain tensor and φ

$$\begin{aligned}\mathcal{H}^{(2)}_{\vec{q}=\vec{0}} &= \int d^2x \, \frac{1}{2}(\mu+\lambda)X_+^2 + \frac{\mu}{2}X_-^2 + 2\mu Y^2 \\ &\quad + g\varphi X_+ + \int d^2x \, \frac{r}{2}\varphi^2,\end{aligned} \tag{A4}$$

where we have defined

$$\begin{aligned}X_+ &= u_{\ell\ell}, \\ X_- &= u_{xx} - u_{yy}, \\ Y &= u_{xy} = u_{yx}.\end{aligned} \tag{A5}$$

The four eigenvalues in this case are given by

$$\begin{aligned}\Lambda_\pm &= \frac{1}{4}\left[B + r \pm \sqrt{(B-r)^2 + 4g^2}\right], \\ \Lambda_1 &= 2\mu, \quad \Lambda_2 = \frac{\mu}{2},\end{aligned} \tag{A6}$$

where $B \equiv \mu + \lambda$. Stability requires $\mu > 0$ and

$$r > g^2/(\mu + \lambda). \tag{A7}$$

Thus, as in a pure elastic theory, the uniform strains impose a more stringent criterion on stability than do the finite-wave-vector modes. Therefore, as temperature is lowered [$r = a_2(T - T_c)$], the uniform mode φ_0 becomes unstable first.

[1] P. Bolhuis, M. Hagen, and D. Frenkel, Phys. Rev. E **50**, 4880 (1994).

[2] P. Bladon and D. Frenkel, Phys. Rev. Lett. **74**, 2519 (1995).

[3] C. F. Tejero, A. Daanoun, H. N. W. Lekkerkerker, and M. Baus, Phys. Rev. E **51**, 558 (1995).

[4] H. Xia, A. L. Ruoff, and Y. K. Vohra, Phys. Rev. B **44**, 10 374 (1991).

[5] E. A. Kamenetzky, L. G. Magliocco, and H. P. Panzer, Science **263**, 207 (1994).

[6] R. J. Hunter, *Foundations of Colloid Science* (Oxford, New York, 1992), Vols. I and II; P. N. Pusey, in *Liquids, Freezing and Glass Transition,* edited by J. P. Hansen, D. Levesque, and J. Zinn-Zustin (North-Holland, Amsterdam, 1991).

[7] T. Chou and D. R. Nelson, Phys. Rev. E **48**, 4611 (1993).

[8] D. H. Van Winkle and C. A. Murray, Phys. Rev. A **34**, 562 (1986); P. Pansu, P. Pieranski, and L. Strzelecki, J. Phys. (Paris) **44**, 531 (1983); see also *Bond Orientational Order,* edited by K. Strandberg (Springer, New York, 1991).

[9] D. Y. C. Chan, J. D. Henry, and L. R. White, J. Colloid Interface Sci. **70**, 410 (1981).

[10] H. N. W. Lekkerkerker and G. J. Vroege, in *Fundamental Problems in Satistical Mechanics VIII,* Proceedings of the 1993 Altenberg Summer School (North-Holland, Amsterdam, 1994).

[11] J. G. Kirkwood, J. Chem. Phys. **7**, 919 (1939).

[12] V. N. Ryzhov and E. E. Tareyeva, Phys. Rev. B **51**, 8789 (1995).

[13] B. J. Alder and T. E. Wainwright, J. Chem. Phys. **27**, 1208 (1958).

[14] M. H. J. Hagen and D. Frenkel, J. Chem. Phys. **101**, 4093 (1994).

[15] A. P. Gast, C. K. Hall, and W. B. Russell, J. Colloid Interface Sci. **96**, 251 (1983).

[16] D. R. Nelson, in *Phase Transitions and Critical Phenomena,* edited by C. Domb and J. Lebowitz (Academic, London, 1984), Vol. 7; K. Strandburg, Rev. Mod. Phys. **60**, 161 (1988); for another presentation of elasticity theory of defects and alternative melting models, see H. Kleinert, *Gauge Fields in Condensed Matter* (World Scientific, Singapore, 1989), Vol. 2.

[17] J. D. Brock, R. J. Birgeneau, J. D. Litster, and A. Aharony, Contemp. Phys. **30**, 321 (1989).

[18] R. Seshadri and R. M. Westervelt, Phys. Rev. B **46**, 5150 (1992); R. Seshadri and R. M. Westervelt, Helv. Phys. Acta (Switzerland) **65**, 473 (1992).

[19] D. S. Fisher, B. I. Halperin, and R. Morf, Phys. Rev. B **20**, 4692 (1979).

[20] K. Chen, T. Kaplan, and M. Mostoller, Phys. Rev. Lett. **70**, 4019 (1995).

[21] A. Jayaraman, Phys. Rev. **137**, A179 (1965); I. G. Zakrevskii, V. V. Kokorin, and V. A. Chernenko, Dokl. Akad. Nauk SSSR **291**, 345 (1986) [Sov. Phys. Dokl. **31**, 911 (1986)]; Yu. V. Knyazev, M. M. Kirillova, Yu. I. Kuzmin, and E. Z. Rivman, Fiz. Nizh. Temp. **17**, 1143 (1991) [Sov. J. Low Temp. Phys. **17**, 559 (1991)].

[22] B. Alder and D. Young, J. Chem. Phys. **70**, 473 (1979).

[23] J. Y. Wang, D. Vaknin, R. A. Uphaus, K. Kjaer, and M. Losche, Thin Solid Films **242**, 40 (1994).

[24] D. R. Nelson and B. I. Halperin, Phys. Rev. B **19**, 2457 (1979).

[25] A. P. Young, Phys. Rev. B **19**, 1855 (1979).

[26] N. Goldenfeld, *Lectures on Phase Transitions and the Renormalization Group* (Addison-Wesley, Reading, MA, 1992); S. K. Ma, *Statistical Mechanics* (World Scientific, Singapore, 1985).

[27] L. D. Landau and E. M. Lifshitz, *Theory of Elasticity* (Pergamon, New York, 1970).
[28] D. J. Bergman and B. I. Halperin, Phys. Rev. B **13**, 2145 (1976).
[29] J. Sak, Phys. Rev. B **10**, 3957 (1974).
[30] D. R. Nelson, Phys. Rev. B **27**, 2902 (1983).
[31] A. Zippelius, B. I. Halperin, and D. R. Nelson, Phys. Rev. B **22**, 2514 (1980).
[32] A. I. Larkin and S. A. Pikin, Zh. Eksp. Teor. Fiz. **56**, 1664 (1969) [Sov. Phys. JETP **29**, 891 (1969)].
[33] M. Kosterlitz and D. J. Thouless, J. Phys. C **6**, 1181 (1973).
[34] J. Prost and J. Toner, Phys. Rev. A **36**, 5008 (1987). These authors find, among other possibilities, an asymmetric droplet of nematic phase near a critical point between two different smectic liquid-crystal phases, similar to the bubble of hexatic phase discussed here. We also expect asymmetric hexatic and modulated hexatic regions near the S_1-S_2 critical point if higher-order terms are included in $\mathcal{H}_{\mathcal{I}}[\varphi]$. However, approaching the critical point (CP), these higher-order terms are negligible and the hexatic bubble becomes symmetric.
[35] D. R. Nelson, Phys. Rev. B **18**, 2318 (1978).